Original Article

Effects of different tube potentials and iodine concentrations on image enhancement, contrast-to-noise ratio and noise in micro-CT images: a phantom study

Hairil Rashmizal Abdul Razak[1], Said Mohd Shaffiq Said Rahmat[1], Wan Mazlina Md Saad[2]

[1]Department of Medical Imaging, [2]Department of Medical Laboratory Technology, Universiti Teknologi MARA, Malaysia

Corresponding to: Hairil Rashmizal Abdul Razak, PhD. Department of Medical Imaging, Faculty of Health Sciences, Universiti Teknologi MARA, 42300 Puncak Alam, Selangor, Malaysia. Email: hairil@puncakalam.uitm.edu.my or rashmizal@yahoo.co.uk.

Abstract: The study aimed to investigate the effects of different tube potentials and concentrations of iodinated contrast media (CM) on the image enhancement, contrast-to-noise ratio (CNR) and noise in micro-computed tomography (μCT) images. A phantom containing of five polyethylene tube was filled with 2 mL of deionized water and iodinated CM (Omnipaque 300 mgI/mL) at four different concentrations: 5, 10, 15, and 20 mol/L, respectively. The phantom was scanned with a μCT machine (SkyScan 1176) using various tube potentials: 40, 50, 60, 70, 80, and 90 kVp, a fixed tube current; 100 μA, and filtration of 0.2 mm aluminum (Al). The percentage difference of image enhancement, CNR and noise of all images, acquired at different kVps and concentrations, were calculated. The image enhancement, CNR and noise curves with respect to tube potential and concentration were plotted and analysed. The highest image enhancement was found at the lowest tube potential of 40 kVp. At this kVp setting, the percentage difference of image enhancement [Hounsfield Unit (HU) of 20 mol/L iodine concentration over HU of deionized water] was 43%. By increasing the tube potential, it resulted with the reduction of HU, where only 17.5% different were noticed for 90 kVp. Across all iodine concentrations (5-20 M), CNR peaked at 80 kVp and then these values showed a slight decreasing pattern, which might be due insufficient tube current compensation. The percentage difference of image noise obtained at 40 and 90 kVp was 72.4%. Lower tube potential setting results in higher image enhancement (HU) in conjunction with increasing concentration of iodinated CM. Overall, the tube potential increment will substantially improve CNR and reduce image noise.

Keywords: Tube potential; iodine concentration; micro-computed tomography (μCT)

Submitted Oct 24, 2013. Accepted for publication Oct 29, 2013.
doi: 10.3978/j.issn.2223-4292.2013.10.04
Scan to your mobile device or view this article at: http://www.amepc.org/qims/article/view/2911/3829

Introduction

Computed tomography (CT) has revolutionized the clinical diagnostic practice by depicting anatomical, physiological, and pathological information (1). However, this readily available CT scanner has not been extensively laboratory investigations of small animals and biomedical research, mainly because of its limitation in spatial resolution (2). The spatial resolution of clinical CT scanner is unable to be scaled down adequately for small animal imaging (3). It can only generate images made up of voxels approximately 1 mm^3 in volume when scanning human while 50 μm^3 volume elements are required when scanning small animal (4). Higher spatial and temporal resolutions are fundamental requirements for anatomical and functional X-ray based imaging (5). The introduction of micro-computed tomography (μCT) scanner in 1990s, has overcome the limitation of clinical CT in small animal studies (6,7) and it has played a critical role in the evolution of molecular imaging (8).

A μCT scanner is built on the similar fundamental physical principle as a clinical CT scanner, but it has been dedicatedly designed for higher quality resolution imaging (5). The system consists of an X-ray source with micro focus spot, a pair of flat panel detector, rotating gantry, a stationary and a horizontally positioned small bed to achieve a cone beam mode scan (9). It is a nondestructive investigation method (10), which has the ability to reconstruct the image slices in any plane from the scans and data can be represented in either 2-dimensional (2D) or rendered in 3-dimensional (3D) images (11). In addition, μCT is capable to perform volumetric CT analyses with isotropic voxel spacing of less than 50 μm (12). The small isotropic voxel spacing can eliminate the need for interpolation between slices when rendering samples in 3D, remove a source of image artifacts and allow for greater versatility during virtual inspection (13). This notable technical advancement have made μCT scanner practicable to obtain such high spatial resolution images of small particles and animals during research investigations (4). Furthermore, a poor inherent subject contrast of μCT images can easily be overcome by using an exogenous contrast media (CM) (14).

CM is radiopaque substances that can be administered intravenously or orally into the body, in order to enhance the radiographical visualization of internal structures (15). Iodinated CM show higher attenuation levels at lower X-ray tube voltage owing to higher photoelectric effect and lesser Compton scattering (16,17). To take benefit of an inherent attenuation property of iodine, the mean photon energy of the tube potential has to be adjusted closer to the k edge of iodine (18). In fact, Szucs-Farkas *et al.* (19) found that the attenuation value of iodine enhancement increased with decreasing in the tube potential and patient size. A study on image quality of μCT images based on the attenuation value of iodine at different tube potential has not yet been well documented. Thus, this gap warrants for further investigations.

Materials and methods

The contrast phantom consisted of four polyethylene tubes were filled with 2 mL of iodinated CM (Omnipaque 300 mgI/mL) at different concentrations: 5, 10, 15, and 20 mol/L, respectively. On the other hand, one control tube was filled with 2 mL of deionized water and all these five tubes were then immersed in a water filled container. The phantom was positioned at the iso-center of the gantry.

μCT scanning

The contrast phantom was scanned using μCT scanner (Skyscan 1176, SkyScan b.v.b.a., Aartselaar, Belgium). The scanning procedure was initially conducted using the following settings: 40 kVp, fixed μA; 100, and filtration of 0.2 mm aluminum (Al). The acquisition consisted of the realization of several 2D lateral projections of the phantom during a 360° rotation around the vertical axis. The scanning protocols were repeated at five different tube potentials: 50, 60, 70, 80, 90 kVp. The set of images were then processed through reconstruction algorithm provided by Skyscan to get the 2D reconstruction of the vials. The digital data were elaborated using reconstruction software (NRecon V1.4.0; SkyScan), which provided new axial cross-sections with a pixel size of 32 μm × 32 μm.

Measurement of contrast noise ratio (CNR) and noise

For each scanning techniques and iodine concentration, the CT number was measured in Hounsfield Unit (HU) from the lowest contrast to highest contrast materials and the background of the phantom. The diameter of all vials are same, thus the size of region of interest (ROI) was kept constant in the purpose of reducing bias in measurements. CNR was calculated as follows (20).

$$\mathrm{CNR} = \frac{ROI_m - ROI_b}{SD_b} \qquad [1]$$

where ROI_m and ROI_b are the CT numbers of the contrast material in a ROI and in the background of ROI, respectively. SD_b is the standard deviation of CT number of the background. Noise was calculated as expressed as (21):

$$Noise = \sqrt{\frac{\sigma_m^2 - \sigma_b^2}{2}} \qquad [2]$$

where σ_m^2 and σ_b^2 are the standard deviation of the target material and the background area that have; same shape and size of ROI. CNR and noise were calculated for each iodine concentration on each set of tube potentials. The measurement was made at the top, middle and bottom slices for the CT numbers and these values were then averaged.

Results

Image in *Figure 1* showed that the variation in image

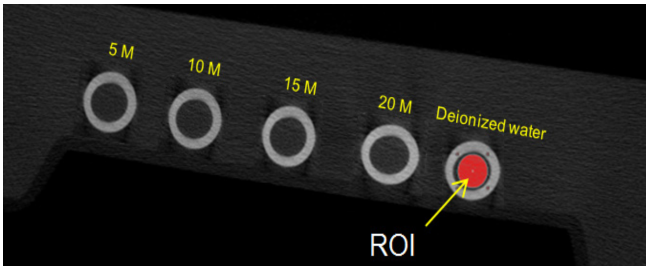

Figure 1 A cross sectional μCT image of contrast phantom containing five vials of 2 mL in volume that has been filled with deionized water and different concentrations of iodinated CM: 5, 10, 15, 20 M. The circle shape of ROI is used for HU measurements. Abbreviations: μCT, micro-computed tomography; CM, contrast media; ROI, region of interest; HU, Hounsfield unit.

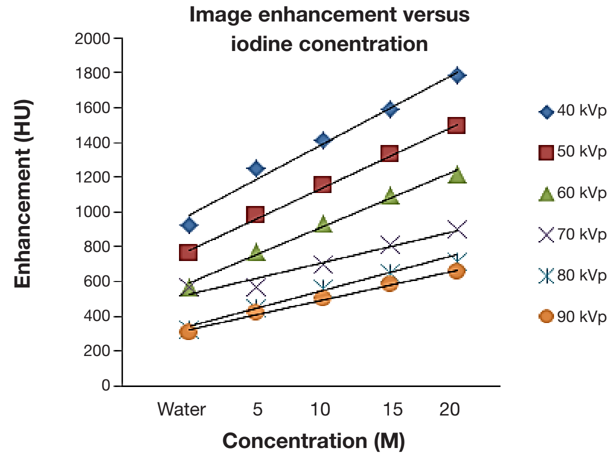

Figure 2 Image enhancement of iodinated CM at different concentration and tube potential setting. Graph shows direct correlation between tube potential and iodine concentration with image enhancement. Abbreviation: CM, contrast media.

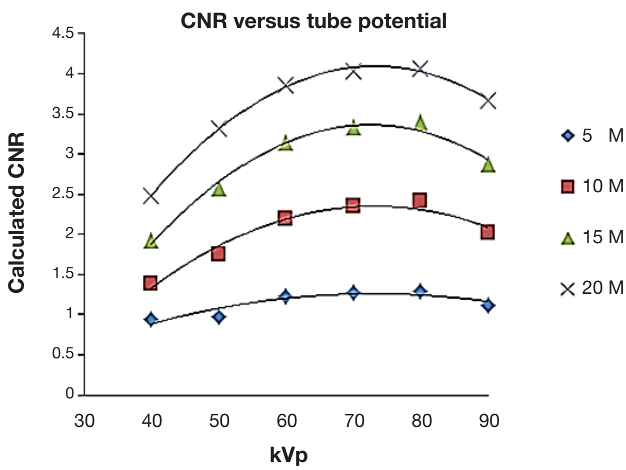

Figure 3 Calculated CNR of iodinated CM at different concentrations and tube potentials setting. Graph shows a slight CNR degradation at 90 kVp. Abbreviations: CNR, contrast-to-noise ratio; CM, contrast media.

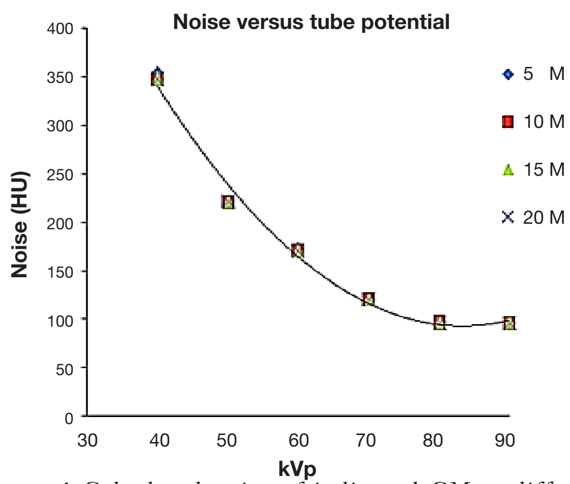

Figure 4 Calculated noise of iodinated CM at different concentrations and tube potentials setting. Graph shows an exponential decreasing pattern of noise from 40-90 kVp. Abbreviation: CM, contrast media.

enhancement between different iodine concentrations in the contrast phantom were depended on the tube potential used. The highest image enhancement was found to be at the lowest tube voltage setting of 40 kVp (*Figure 2*). At this kVp setting, the percentage difference of image enhancement in HU of 20 M iodine concentration over HU of deionized water was 43%. By increasing the tube potential, it resulted in a reduction of image enhancement, where only 17.5% different were noticed for 90 kVp. Higher concentration of iodinated CM demonstrate greater contrast enhancement than the lower concentration of iodinated CM at low tube potentials.

Across all iodine concentration from 5 to 20 M, the CNR increases along with the increment of the tube potential. This trend continues until its peak at 80 kVp (*Figure 3*). The percentage differences of CNR at lower to higher concentrations of iodine at 40 and 80 kVps were 38.7% and 64.4%, respectively. However, above 80 kVp, the CNR values showed a slight decreasing pattern, which might be due to insufficient tube current compensation. As expected, the image noise was inversely related with the tube potential (*Figure 4*). At a fixed tube current, the lowest and the highest noise were seen at 90 and 40 kVp, with the percentage difference of 72.4%. Besides, with increasing the tube potential and iodine concentration, noise exponentially decreased. At same tube potential the differences in noise variation decreased; the noise value was constant across all iodine concentrations.

Discussions

The degree of contrast enhancement is directly related to the amount of iodine within the system and the level of tube potential, where contrast enhancement increases proportionally with iodine concentration (22). Our findings are in accordance with a previous study, where CT attenuation value of iodine increased at lower tube potential and resulted in higher image enhancement (19). The potential explanation for this phenomenon would be referred to the photoelectric effect (17). At a lower tube potential, the influence of the photoelectric interactions in the present of iodinated CM is greater compared with Compton scattering effects because of the 33-keV k-edge of iodine (23). As a consequence, it leads to an increase in the linear attenuation coefficient of iodine much more dramatically than water and this offers superior contrast enhancement (24).

On the other hand, higher concentration of iodinated CM provide significantly greater contrast enhancement compared with those of lower concentration, which mainly due to higher production of signal intensity on the detector (25). The present study seems to be in consistent with previous reported data on CT angiography (CTA) of renal arterial vessels where the usage of highly concentrated iodinated CM at lower tube potential demonstrated higher contrast enhancement compared to moderate concentration (26). Even though higher concentration of iodinated CM improves contrast enhancement, but it results in increased osmolality which may cause higher risk of contrast induced adverse reactions (27). In addition, an excessive concentration of iodinated CM can lead to beam hardening artifacts and directly degrade the image quality produced (28).

This study demonstrated that CNR increased with the increment of tube potentials and iodine concentrations. It is in accordance with previous phantom study where the CNR was increased by factor of up to 3.6 when increasing tube potential from 80 to 140 kVp (29). Although our data have shown that increment of the tube potential improves the CNR, this does not necessarily imply that μCT should be performed at the highest possible kVp value. Higher tube potential could increase the radiation dose as a result of exposure to higher X-ray energies (30). It is also important to note that if the image quality at lower tube potential is adequate to achieve a high level of diagnostic accuracy, then any improvement in CNR would not be further translated towards improving diagnostic performance (29).

Scanning with lower tube potential will result in increasing noise caused by direct reduction in photon flux (31). Lower tube potential scans produce smaller number of photon strike the detector and thus results in limited data to construct an optimum image. These inadequate amounts of constructed data may cause the image appear to be very grainy (32) and influence the diagnostic value of images (29). Our study demonstrated that image noise exponentially decreased with the increment of tube potential. The percentage difference of image noise obtained at 40 and 90 kVp was 72.4%. It is consistent with those previously reported data on CTA of the aorta where a 35% increment of image noise was noted with the 100 kVp protocol in comparison with the 120 kVp protocol by using constant level of tube current (33). The usage of higher concentration of iodinated CM was able to reduce image noise (34). On the contrary, our study showed almost unchanged level of image noise across all iodine concentrations at same tube potential. Image noise is closely related to tube current and tube potential, where both of these parameters determine the photon fluency and incident beam energy (35). In order to compensate image noise when decreasing the tube potential, the tube current needs to be increased. Therefore, an appropriate selection of scanning parameter is critical in obtaining optimum image quality as well as radiation exposure (36).

This study has its own limitation, where the investigation only focused on manipulation of tube potential setting but did not take into account the manipulation of tube current. Image quality and examination efficiency of CT scan depend on the tube current setting (37); decreasing tube current produces lower sampling rate with resultant lower image quality and higher image noise. Future work should include the tube current investigation, therefore the optimum tube current setting can be selected with reference to tube potential in the purpose of reducing image noise and improving image quality.

Conclusions

This phantom study shows that μCT scanning with lower tube potential setting yields higher image enhancement

(HU) in conjunction with increasing concentration of iodinated CM although the image noise is increased. Overall, CNR substantially improves when tube potential setting and iodine concentrations are increased. By utilizing these unique scanning techniques (low kVp and high iodine concentration), a better quality of µCT images could therefore be produced; without CNR degradation.

Acknowledgements

The authors would like to acknowledge the Research Management Institute (RMI) of Universiti Teknologi MARA, Shah Alam, Malaysia for the RAGS grant awarded [600-RMI/RAGS 5/3/(119/2012)].
Disclosure: The authors declare no conflict of interest.

References

1. Alfidi RJ, Haaga J, Meaney TF, et al. Computed tomography of the thorax and abdomen; a preliminary report. Radiology 1975;117:257-64.
2. Batiste DL, Kirkley A, Laverty S, et al. High-resolution MRI and micro-CT in an ex vivo rabbit anterior cruciate ligament transection model of osteoarthritis. Osteoarthritis Cartilage 2004;12:614-26.
3. Ritman EL. Micro-computed tomography of the lungs and pulmonary-vascular system. Proc Am Thorac Soc 2005;2:477-80, 501.
4. Holdsworth DW, Thornton MM. Micro-CT in small animal and specimen imaging. Trends Biotechnol 2002;20:S34-9.
5. Badea CT, Drangova M, Holdsworth DW, et al. In vivo small-animal imaging using micro-CT and digital subtraction angiography. Phys Med Biol 2008;53:R319-50.
6. Kuhn JL, Goldstein SA, Feldkamp LA, et al. Evaluation of a microcomputed tomography system to study trabecular bone structure. J Orthop Res 1990;8:833-42.
7. Vaquero JJ, Redondo S, Lage E, et al. Assessment of a new High-Performance Small-Animal X-Ray tomograph. IEEE Trans Nucl Sci 2008;55:898-905.
8. Paulus MJ, Gleason SS, Kennel SJ, et al. High resolution X-ray computed tomography: an emerging tool for small animal cancer research. Neoplasia 2000;2:62-70.
9. Kim KW, Kim KG, Kim JH, et al. Development of the 3D volumetric micro-CT scanner for preclinical animals. 3D Res 2011;2:1-6.
10. Stoico R, Tassani S, Perilli E, et al. Quality control protocol for in vitro micro-computed tomography. J Microsc 2010;238:162-72.
11. Spagnuolo G, Ametrano G, D'antò V, et al. Microcomputed tomography analysis of mesiobuccal orifices and major apical foramen in first maxillary molars. Open Dent J 2012;6:118-25.
12. Voor MJ, Yang S, Burden RL, et al. In vivo micro-CT scanning of a rabbit distal femur: repeatability and reproducibility. J Biomech 2008;41:186-93.
13. Rutty GN, Brough A, Biggs MJ, et al. The role of micro-computed tomography in forensic investigations. Forensic Sci Int 2013;225:60-6.
14. Prajapati SI, Keller C. Contrast enhanced vessel imaging using microCT. J Vis Exp 2011;(47):2377.
15. Ehrlich RA, Daly JA. Patient Care in Radiography: with an Introduction to Medical Imaging (Ehrlich, Patient Care in Radiography). Mosby, 2004.
16. Bahner ML, Bengel A, Brix G, et al. Improved vascular opacification in cerebral computed tomography angiography with 80 kVp. Invest Radiol 2005;40:229-34.
17. Nakayama Y, Awai K, Funama Y, et al. Abdominal CT with low tube voltage: preliminary observations about radiation dose, contrast enhancement, image quality, and noise. Radiology 2005;237:945-51.
18. Schindera ST, Nelson RC, Mukundan S Jr, et al. Hypervascular liver tumors: low tube voltage, high tube current multi-detector row CT for enhanced detection--phantom study. Radiology 2008;246:125-32.
19. Szucs-Farkas Z, Verdun FR, von Allmen G, et al. Effect of X-ray tube parameters, Iodine concentration, and patient size on image quality in pulmonary computed tomography angiography: a chest-phantom-study. Invest Radiol 2008;43:374-81.
20. Funama Y, Awai K, Nakayama Y, et al. Radiation dose reduction without degradation of low-contrast detectability at abdominal multisection CT with a low-tube voltage technique: phantom study. Radiology 2005;237:905-10.
21. Song X, Pogue BW, Jiang S, et al. Automated region detection based on the contrast-to-noise ratio in near-infrared tomography. Appl Opt 2004;43:1053-62.
22. Bae KT. Intravenous contrast medium administration and scan timing at CT: considerations and approaches. Radiology 2010;256:32-61.
23. Murakami Y, Kakeda S, Kamada K, et al. Effect of tube voltage on image quality in 64-section multidetector 3D CT angiography: Evaluation with a vascular phantom with superimposed bone skull structures. AJNR Am J Neuroradiol 2010;31:620-5.
24. Yu L, Bruesewitz MR, Thomas KB, et al. Optimal

tube potential for radiation dose reduction in pediatric CT: principles, clinical implementations, and pitfalls. Radiographics 2011;31:835-48.
25. Silvennoinen HM, Hamberg LM, Valanne L, et al. Increasing contrast agent concentration improves enhancement in first-pass CT perfusion. AJNR Am J Neuroradiol 2007;28:1299-303.
26. Cho ES, Yu JS, Ahn JH, et al. CT angiography of the renal arteries: comparison of lower-tube-voltage CTA with moderate-concentration iodinated contrast material and conventional CTA. AJR Am J Roentgenol 2012;199:96-102.
27. Maddox TG. Adverse reactions to contrast material: recognition, prevention, and treatment. Am Fam Physician 2002;66:1229-34.
28. Campbell C, Lubner MG, Hinshaw JL, et al. Contrast media-doped hydrodissection during thermal ablation: optimizing contrast media concentration for improved visibility on CT images. AJR Am J Roentgenol 2012;199:677-82.
29. Huda W, Scalzetti EM, Levin G. Technique factors and image quality as functions of patient weight at abdominal CT. Radiology 2000;217:430-5.
30. Nicol E, Stirrup J, Kelion AD, et al. Cardiovascular Computed Tomography. Oxford: Oxford University Press, 2011.
31. Tang K, Wang L, Li R, et al. Effect of low tube voltage on image quality, radiation dose, and low-contrast detectability at abdominal multidetector CT: phantom study. J Biomed Biotechnol 2012;2012:130169.
32. Webb WR, Brant WE, Major NM. Fundamentals of body CT. 3rd ed. Philadelphia: Elsevier Saunders, 2006:309-10.
33. Wintersperger B, Jakobs T, Herzog P, et al. Aorto-iliac multidetector-row CT angiography with low kV settings: improved vessel enhancement and simultaneous reduction of radiation dose. Eur Radiol 2005;15:334-41.
34. Iezzi R, Santoro M, Marano R, et al. Low-dose multidetector CT angiography in the evaluation of infrarenal aorta and peripheral arterial occlusive disease. Radiology 2012;263:287-98.
35. Tack D, Kalra MK, Gevenois PA. Radiation Dose from Multidetector CT. Springer, 2012.
36. Lee JKT. Computed Body Tomography With MRI Correlation. Lippincott Williams & Wilkins, 2006.
37. Terrier F, Grossholz M, Becker CD. Spiral CT of the Abdomen. Springer-Verlag GmbH & Co. KG, 2000.

Cite this article as: Abdul Razak HR, Shaffiq Said Rahmat SM, Md Saad WM. Effects of different tube potentials and iodine concentrations on image enhancement, contrast-to-noise ratio and noise in micro-CT images: a phantom study. Quant Imaging Med Surg 2013;3(5):256-261. doi: 10.3978/j.issn.2223-4292.2013.10.04